Pharm Res (2014) 31:1264–1274
DOI 10.1007/s11095-013-1247-5

RESEARCH PAPER

Targeting Tamoxifen to Breast Cancer Xenograft Tumours: Preclinical Efficacy of Folate-Attached Nanoparticles Based on Alginate-Cysteine/Disulphide-Bond-Reduced Albumin

A. Martínez • E. Muñiz • C. Teijón • I. Iglesias • J. M. Teijón • M. D. Blanco

Received: 27 July 2013 / Accepted: 20 October 2013 / Published online: 12 November 2013

ABSTRACT

Purpose *In vivo* evaluation of tamoxifen (TMX)-loaded folate-targeted nanoparticles prepared from a mixture of disulphide bond reduced bovine serum albumin (BSA-SH) and alginate-cysteine (ALG-CYS) as targeted delivery systems of TMX to tumour tissues.

Methods TMX in solution, TMX included into folate-nanoparticles and their non-targeted analogues were intravenously administered to nude mice carrying xenograft MCF-7 tumours. The antitumor activity of these systems was characterized in terms of tumour growth rate, histological and immunohistochemical analysis of tumour tissues and TMX biodistribution.

Results TMX-folate-attached nanoparticles caused tumour remission whereas free TMX or TMX-non-targeted nanoparticles could only stop the tumour development. The histological evaluation of tumour tissues showed that those treated with folate-conjugated systems presented the most quiescent and disorganized structures. Additionally, the lowest concentrations of TMX accumulated in non-targeted organs were also found after administration of the drug using this formulation.

Conclusions This study demonstrated that TMX-loaded folate-targeted systems were capable of reaching tumour sites, so enhancing the *in vivo* anticancer action of TMX, and allowing a new administration route to be applied and some of the current TMX therapy problems to be overcome.

KEY WORDS folic acid · nanoparticles · natural polymers · tamoxifen · targeted breast cancer therapy

ABBREVIATIONS

ALG-CYS	Alginate-cysteine conjugate
ANOVA	One way analysis of variance
BSA	Bovine serum albumin
BSA-SH	Disulphide bond reduced bovine serum albumin
B-50-50 NP	Nanoparticles based on 50% ALG-CYS and 50% BSA-SH
B-50-50-FOL NP	Folate-conjugated nanoparticles based on 50% ALG-CYS and 50% BSA-SH
DCC	*N*,*N*′-dicyclohexylcarbodiimide
DMSO	Dimethyl sulphoxide
EDTA	Ethylenediaminetetraacetic acid
FBS	Foetal bovine serum
i.v	Intravenous administration
KCl	Potassium chloride
NaCl	Sodium chloride
NaOH	Sodium hydroxide
NP	Nanoparticles
PBS	Phosphate buffered saline
s.c	Subcutaneous administration

A. Martínez • I. Iglesias
Departamento de Farmacología Facultad de Farmacia
Universidad Complutense de Madrid Madrid, Spain

E. Muñiz
Departamento de Biología Celular Facultad de Biológicas
Universidad Complutense de Madrid Madrid, Spain

C. Teijón
Departamento de Enfermería Escuela Universitaria de Enfermería
Fisioterapia y Podología, Universidad Complutense de Madrid
Madrid, Spain

J. M. Teijón • M. D. Blanco
Departamento de Bioquímica y Biología Molecular
Facultad de Medicina, Universidad Complutense de Madrid
Madrid, Spain

M. D. Blanco (✉)
Departamento de Bioquímica y Biología Molecular, Pabellón IV
Facultad de Medicina, Universidad Complutense de Madrid
Avda. Complutense s/n, 28040 Madrid, Spain
e-mail: mdblanco@med.ucm.es

TMX- B-50-50-FOL NP	Tamoxifen-loaded folate-conjugated nanoparticles based on 50% ALG-CYS and 50% BSA-SH
TMX- B-50-50 NP	Tamoxifen-loaded nanoparticles based on 50% ALG-CYS and 50% BSA-SH
4-OH-TMX	4-hydroxytamoxifen

INTRODUCTION

Targeting emerges as a new strategy to make drug delivery more specific, in that it allows more localised drug administration to be achieved and reduces the development of undesirable side effects derived from unspecific drug accumulation (1). The promising possibilities that drug targeting strategies have to offer are of notable importance in the case of cancer therapy, where the majority of anticancer treatments cause toxic side effects which considerably affect a patient's quality of life. With these new challenging opportunities we are able to face some problematic issues of cancer management, and to design personalized therapies that cause less adverse effects (2).

Advanced or metastatic breast cancer has been treated for more than 20 years with TMX (3), a selective oestrogen-receptor modulator (SERM), which presents certain limitations, such as low solubility in water, which forces its oral administration, and some important side effects, like endometrial cancer development due to its oestrogen-agonist role in the uterus. Thus, the vectorization of TMX therapy could overcome some of these problems and would enhance the efficacy of this drug.

The functionalization of nanoparticle surfaces with biomolecules that interact with specific receptors over-expressed in targeted cells is an useful approach to achieve drug targeting at the cellular level (4). Folic acid is a common ligand frequently used in targeting strategies due to the over-expression of folate receptors (FR) in several types of human cancer cells (e.g. prostate, ovarian and breast cancer cells) and its high binding affinity for FR (FR, $K_d \sim 10^{-10}$ M) (5). Additionally, folic acid offers a ligand-activated endocytosis pathway for drugs, such as TMX, that need to be internalized by cells in order to carry out their function (6).

Tamoxifen-loaded nanoparticles prepared from several mixtures of thiolated-alginate (ALG-CYS) and modified albumin (BSA-SH) have been shown to be good candidates for use as controlled delivery systems, either *in vitro* (7,8) or *in vivo* (9), where TMX antitumor efficacy was enhanced following their subcutaneous administration.

In this study, the anticancer activity of TMX-loaded folate-targeted nanoparticles, which have recently been characterized *in vitro* (10), was evaluated by using a xenograft breast cancer model developed in nude mice by intravenous administration, and by comparing their anticancer action to their non folate-targeted analogue nanoparticles and to TMX administered free in solution.

MATERIALS AND METHODS

Materials

Folic acid, alginic acid sodium salt (viscosity 200.00–400.000 cps), tamoxifen (TMX), 4-hydroxytamoxifen (4OH-TMX), 17-β-estradiol valerate, sesame oil, *N*-hydroxysuccinimide (NHS), *N*,*N*′-dicyclohexylcarbodiimide (DCC), gentamicin (50 μg/ml), dimethyl sulphoxide (DMSO) and paraformaldehyde were purchased from Sigma-Aldrich (Barcelona, Spain). Sodium hydroxide (NaOH), hydrochloric acid (HCl; 37%), absolute ethanol, xylene, acetonitrile, triethylamine, tris(hydroxymethyl) aminomethane and potassium dihydrogenphosphate were purchased from Panreac (Barcelona, Spain). Bovine serum albumin (BSA, Fraction V) and dehydrated disodium hydrogen phosphate were purchased from Merck (Barcelona, Spain). Foetal bovine serum (FBS), penicillin (50 U/ml), streptomycin (50 μg/ml), L-glutamine (200 mM) and 0.05% trypsin/0.53 mM EDTA were purchased from Invitrogen Life Technologies (Grand Island, NY, USA). Dulbecco's modified Eagle medium was purchased from Lonza (Belgium).

Preparation of Non-folate-Conjugated Nanoparticles

Non folate-conjugated nanoparticles based on a mixture of BSA-SH and ALG-CYS were prepared following the protocol described in previous works (7). Briefly, disulphide bonds of BSA were reduced with 2-mercaptoethanol to prepare BSA-SH, and L-cysteine molecules were attached to the alginate structure using a carbodiimide-mediated reaction to synthesized ALG-CYS conjugate. (8). Then, 100 mg BSA-SH and 100 mg ALG-CYS were dissolved in 20 ml 1 mM HCl with vigorous stirring. The suspension was sonicated (Branson sonifier 450) and the pH was raised to 6.5–6.8 with 1 M NaOH. The reaction proceeded for 12 h under vigorous stirring.5 ml of a solution of L-cysteine (0.06 mM) were then added and the reaction was maintained for a further 5 h to block residual free thiol groups. After this time the resulting suspension was centrifuged (41000 rpm, 15 min, Beckman Coulter Optima L-100 XP Ultracentrifuge), and the nanoparticles (B-50-50 NP) were freeze dried for 24 h at −110°C. As previous studies indicated, the final BSA-SH/ALG-CYS ratio in the nanoparticle composition was 1.16/1 (8).

Preparation of Folate-Conjugated Nanoparticles

Folate-conjugated B-50-50 nanoparticles (B-50-50-FOL NP) were prepared according to the method carried out in previous studies (10). Briefly, NHS-folate (50 mg), obtained by following the protocol developed by Lee and Low (11) was dissolved in 1.0 ml DMSO and added slowly to 2 ml of the stirred nanoparticle suspension (10 mg NP/ml, while the pH was adjusted to 10 using 1 M carbonate/bicarbonate buffer). After stirring for 45 min at room temperature the reaction mixture was centrifuged and washed (41000 rpm, 20 min) to separate unreacted folic acid and other by-products. Finally, B-50-50-FOL nanoparticles were freeze dried for 24 h at −110°C.

Preparation of Tamoxifen-Loaded Nanoparticles

B-50-50 NP and B-50-50-FOL NP were loaded with tamoxifen following the protocol described in a previous work (7). Briefly, 20 mg B-50-50 NP and 20 mg B-50-50-FOL NP were suspended in 1 ml 500 μg/ml TMX solution (in ethanol), and incubated for 12 h at room temperature. The suspensions were then centrifuged (41000 rpm, 15 min) and the nanoparticles were again freeze-dried. TMX-B-50-50 NP and TMX-B-50-50-FOL NP were obtained and, together with their respective unloaded nanoparticles, were used for the *in vivo* studies. Some of their physicochemical characteristics, which were determined in previous works (7,10), have been collected in Table I.

Cell Culture

Human breast adenocarcinoma MCF-7 cells were obtained from Dr. von Kobbe (Chimera Pharma of Bionostra group), whose original source was ATCC® and between 20 and 25 passage numbers. The folate receptor expression in this cell line was previously assessed (10), and a Fluorescent Index FI = 8.9 was obtained. The cells were maintained in Dulbecco's modified Eagle medium, supplemented with 10% heat inactivated FBS, penicillin (50 U/ml), streptomycin (50 μg/ml), L-glutamine (200 mM) and gentamicin (50 μg/ml) in an humidified incubator at 37°C and 5% CO_2 atmosphere (HERA cell, Sorvall Heraeus, Kendro Laboratory Products Gmbh, Hanau, Germany). The cells were plated in a 75-cm^2 flask (Sarstedt Ag and Co., Barcelona, Spain) and were passaged when reaching 95% confluence, by gentle trypsinization. For inoculation into nude mice, the cells were suspended in DMEM prior to injection.

Animals and Implantation of Tumour Cells

The implantation of tumour cells into animals in order to develop palpable tumours was carried out in accordance with the following protocol, which was approved by the Animal Experimentation Ethics Committee of Complutense University of Madrid, and which had already been utilised in a previous work (9). Briefly, four-week-old female nu/nu athymic nude mice (Harlan Inc, Indianapolis, IN, USA) were maintained under sterile conditions with food and water *ad libitum*. Cultured cells (10^7 cells/0.3 ml DMEM) were inoculated subcutaneously into the right flank of each mouse though a 23-G needle under isofluran anaesthesia conditions. 17-β estradiol valerate s.c. injections (50 μg in 0.1 ml sesame oil) were performed immediately after cell transplantation and repeated once a week to sustain tumour growth (12). After the development of palpable solid tumours (~ 400 mm^3), hormonal treatment was stopped and the mice were divided into six groups of five each: untreated mice (saline serum); mice treated with 5 mg/ml placebo B-50-50 NP and B-50-50-FOL NP (drug-unloaded); mice treated with 20 μg/ml free tamoxifen, and mice treated with 5 mg/ml TMX-B-50-50 NP and TMX-B-50-50-FOL NP (eq. to 4 μg tamoxifen). Intravenous injections (200 μl) were administered through the tail vein every 3 days over 12 days.

Since very different tumour volumes were obtained before the start of each treatment, the groups were organized according to the following criterion: the biggest and the most vascularised tumours were selected for the formation of TMX treatment groups (free TMX and TMX-loaded NP) becauseTMX treatment was expected to slow down tumour growth and might avoid an excessive tumour growth, which could imply the sacrifice of those mice. The smallest tumours were reserved for control and unloaded-NP groups, because it

Table I Physicochemical Characteristics of the Nanoparticles Used in the *in vivo* Study

	Mean size (nm)	Zeta potential (mV)	Folic acid content (μmol/g NP)	Amount of TMX loaded (μg/mg NP)	Uptake of Coumarin-loaded NP by MCF-7 cells at 24 h (μg NP/cm^2)
B-50-50 NP	449 [7]	−50 ± 6 [7]	–	–	13 ± 1 [10]
B-50-50-FOL NP	68 [10]	−23.4 ± 0.6 [10]	143 ± 25 [10]	–	36 ± 7 [10]
TMX-B-50-50 NP	446 [7]	−37 ± 9 [7]	–	4.1 ± 0.6 [7]	–
TMX-B-50-50-FOL NP	76 [7]	42 ± 2 [10]	143 ± 25 [10]	4.2 ± 0.3 [10]	–

Values in square brackets correspond to the number of the reference

was hypothesized that those treatments would not have any effect on tumour growth. Thus, tumours could continue growing without sacrificing any animal due to excessive tumour size. Additionally, mice with similar tumour volumes were selectively grouped together to diminish intra-group standard deviation.

Tumour size was evaluated every three days and its value was estimated using the following equation: tumour volume = $0.5 \times (W^2 \times L)$, where W is the smaller perpendicular diameter and L is the larger perpendicular diameter. Following completion of the treatment schedule, the mice were sacrificed. The tumours were isolated, and sections of these were taken and fixed in paraformaldehyde 4%. The remaining tumour samples, together with selected extracted organs (liver, lungs, uterus and ovaries, spleen and kidneys) and plasma samples, were frozen for later TMX quantification studies.

Tumour Histology and Immunohistochemistry Studies

Tumours were washed in ethanol and xylene after the fixation step, and embedded in Paraplast® (Surgipath®, Leica). They were then cut for both histological observation (9) using toluidine blue and hematoxylin-eosin staining methods (13), and for inmunohistochemical studies, using the Ki-67 labelling test (9,14). The presence of Ki-67 was determined using a purified mouse anti-human Ki-67 primary antibody (1:25, BD Biosciences Pharmingen, USA), which was after revealed using a secondary antibody attached to a fluorescence dye (Rabbit anti-mouse rhodamine-conjugated as second antibody, 1:1000, Aviva Systems Biology). Some tissue sections were treated only with the second antibody and were used as negative controls to ensure specific staining of the Ki-67 positive cells.

Quantification of Tamoxifen and 4-Hydroxytamoxifen in Plasma and Tissues

The biodistribution of TMX and its metabolite, 4-hydroxytamoxifen (4OH-TMX), in several organs and tissues from treated mice was determined following the protocol developed in previous studies (9). Briefly, liver, lungs, uterus and ovaries, spleen, kidneys and tumour samples were homogenized (Heidoloph RZR 2050 electronic) at 1200 rpm in ice-cold 50 mM Tris–HCl buffer, pH 7.4. The homogenates and plasma samples were mixed with an equal volume of acetonitrile and then centrifuged at 13250 rpm for 6 min. The supernatants were analyzed by high performance liquid chromatography using a fluorescence detector (15). Standard solutions (5–500 ng/ml) of TMX and 4OH-TMX in acetonitrile/water (50/50, v/v) were used to obtain the calibration curves, and a good linear correlation ($r^2 = 0.99$) was obtained.

Statistical Analysis

Results were expressed as the mean ± standard deviation (SD). Statistical analysis was performed using one way analysis of variance (ANOVA) following by Bonferroni post-hoc analysis with computer software SPSS 19.0. A P-value < 0.05 and $P < 0.01$ was considered significant and very significant, respectively.

RESULTS

Tumour Evolution Analysis

The anticancer activity of TMX-loaded nanoparticles was evaluated comparatively to the activity of TMX in solution and the placebo NP using a MCF-7 xenograft nude mice model.. All treatments were well tolerated since none of the treatment groups showed significant weight loss (data not shown).

Tumour volume was measured every 3 days over 36 days to observe the tumour evolution of each group (Fig. 1). Two values of tumour growth rate were then determined for each treatment group (Table II): the first was calculated considering the period of time before treatment started (V_1); the second was determined from the beginning of the treatment until the end of the experiment (V_2). The V_2/V_1 ratio was then calculated for each group (Table II).

As it can be observed in Fig. 1a, control and unloaded-NP treated groups displayed tumours with ever increasing volumes until the end of the experiment. They showed similar V_1 values but different V_2 values. Consequently, different V_2/V_1 ratios were obtained for each group (Table II). In the case of the control group V_1 and V_2 were equal, meaning that serum saline injections did not affect tumour growth rate during the whole experiment. However, the treatment with unloaded B-50-50 NP and, especially, with B-50-50-FOL NP caused a stimulation of tumour growth, since both ratios V_2/V_1 were >1 (Table II).

Regarding the TMX-treated groups, similar tumour volumes were detected for TMX-B-50-50-FOL NP and free TMX groups before treatment started, with similar V_1 values (Table II), while TMX-B-50-50 NP treated mice showed the highest V_1 value. Despite these different values of tumour growth rate before treatment administration, the three groups showed lower V_2 values than their respective V_1, and even a negative V_2 value was obtained in the case of TMX-B-50-50-FOL NP group (Table II). This fact indicated that TMX-B-50-50-FOL NP treatment caused the remission of tumours from the first day of the treatment (Fig. 1), since significantly lower ($p < 0.05$) tumour volume values were found at day 27 and 33 than at day 24, when the treatment started. Meanwhile, either free TMX or TMX-B-50-50 NP treatment slowed down the tumour evolution from the start of

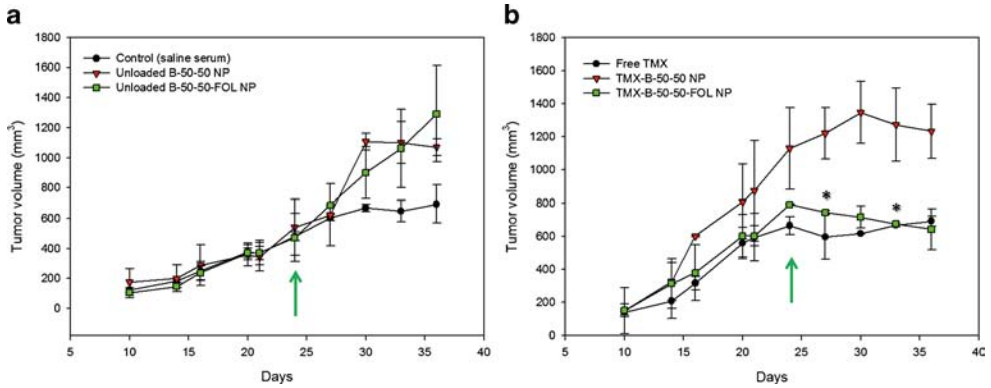

Fig. 1 Tumour evolution of control and placebo nanoparticles treated groups (**a**) compared with TMX-loaded NP and free TMX treated groups (**b**). Green arrows indicate the day of the treatment start (day 24) following the development of palpable tumours in mice. The values are expressed as the mean ± standard deviation ($n = 5$). Data marked with * showed significant ($p < 0.05$) statistical differences with regard of the tumour volume value at day 24.

these treatments. In the case of free TMX, tumour volume continued increasing slowly until the end of the experiment. But in the case of TMX-B-50-50 NP treatment, the tumour volume seemed to start diminishing from day 30, and the rate of tumour growth was calculated to be negative (V_3) (Table II). Nevertheless, significant differences ($p > 0.05$) were not found in this case between tumour values at day 33 and 36 with respect to that one at day 30.

The results indicated that the administration of TMX incorporated in TMX-B-50-50-FOL NP was the most effective treatment compared to TMX administered in a free state or TMX trapped in non-targeted NP.

Tumour Histology and Immunohistochemistry Studies

Histological analysis of tumour tissues from TMX-treated and untreated mice was performed as shown in Fig. 2a. The control tumour cuts showed polyhedral cells, where nuclei containing dispersed chromatin and prominent nucleoli were present. These tissues showed high mitotic activity, since the cells were frequently seen in different phases of division (Fig. 2a). Similar conclusions were extracted from the hematoxylin-eosin stain (Fig. 3a). The appearance of tumour cuts treated with unloaded nanoparticles, either B-50-50 NP or B-50-50- FOL NP, resulted in very similar images to those obtained from the control group. Consequently, the same conclusions about these tissues were arrived at(pictures not shown). In the case of TMX-treated tumours, clear differences could be observed compared to untreated tumours. More highly disorganized and retracted tissues with poorly defined cells and low mitotic activity are to be seen in Figs. 2(b, c and d) and 3(b, c and d). This fact became much more noticeable in the case of tumours treated with TMX-B-50-50-FOL NP, which presented the most disorganized structure (Fig. 2c) showing areas with high cellular adhesion and cellular contraction. Furthermore, mitoses were mostly absent, not only in Fig. 2c but also in Fig. 3c. Although free TMX and TMX-B-50-50 NP exerted a considerable antitumor activity on tumour tissues, the treatment with TMX-B-50-50-FOL NP seemed to be much more effective. In fact, some residual nanoparticles were detected inside TMX-B-50-50-FOL NP treated tumour samples stained by toluidine-blue, as Fig. 4 illustrates.

Additionally, a Ki-67 cell proliferation assay was carried out to differentiate proliferating cells from dead cell populations in the tissues. As Fig. 5 shows, the highest fluorescent signal was obtained in the case of tumours from control group (5B), especially in the central area of the tumour section, where more blood vessels were located. Similar results

Table II Tumour Growth Rates During the Treatment Period and Tumour Growth Ratios of Different Groups

Tumour growth rate and tumour growth ratio			
Group of treatment	Before treatment start: 10–24 days (V_1) (mm^3/day)	After treatment start: 24–36 days (V_2) (mm^3/day)	V_2/V_1 Ratio
Control (saline serum)	25 (0.961)[a]	25 (0.961)[a]	1
Unloaded B-50-50 NP	26 (0.929)[a]	46 (0.991)[a]	1.7
Unloaded B-50-50-FOL NP	27 (0.972)[a]	67 (0.998)[a]	2.4
TMX-loaded B-50-50 NP	70 (0.983)[a]	d24-d30: 36 (0.991)[a] (V_2)	V_2/V_1: 0.5
		d30-d36: -19 (0.970)[a] (V_3)	V_3/V_2: -0.5
TMX-loaded B-50-50-FOL NP	46 (0.990)[a]	−12.36 (0.995)[a]	−0.3
Free TMX	42 (0.960)[a]	11.39 (0.970)[a]	0.3

[a] Value in parenthesis is r^2

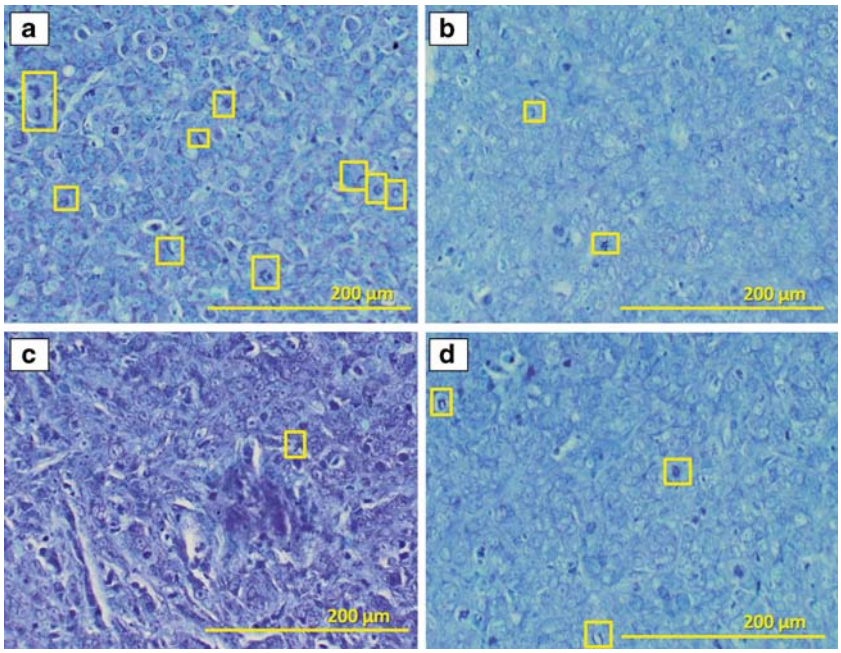

Fig. 2 Histological appearance of the epithelial-like cortex of MCF-7 cell untreated tumour (**a**), TMX-B-50-50 NP treated tumour (**b**), TMX-B-50-50-FOL NP treated tumour (**c**) and free TMX treated tumour (**d**), using the toluidine blue staining method (magnification 40X). Boxes indicate the presence of cells in different stages of mitotic division. *Yellow* bars represent 200 μm.

were obtained in the case of tumours treated with placebo NP (pictures not shown). In contrast, low fluorescent signals were observed in the tumours from TMX-treated groups (E, H, K), meaning that the presence of the antigen in these tissues was significantly reduced and that TMX was exerting its anticancer action. However, the lowest fluorescent signal was detected when TMX was administered trapped in TMX-B-50-50-FOL NP (Fig. 5h), even in the areas surrounding the blood vessels. It would appear that, as a consequence, the number of proliferating cell populations was noticeably reduced due to the enhanced antitumor activity of TMX when it was included in folate-targeted NP. This agreed with the results obtained in the histological study.

Quantification of Tamoxifen and 4-Hydroxytamoxifen in Plasma and Tissues

The concentration of TMX and 4OH-TMX was determined in plasma and organ samples to study possible differences in

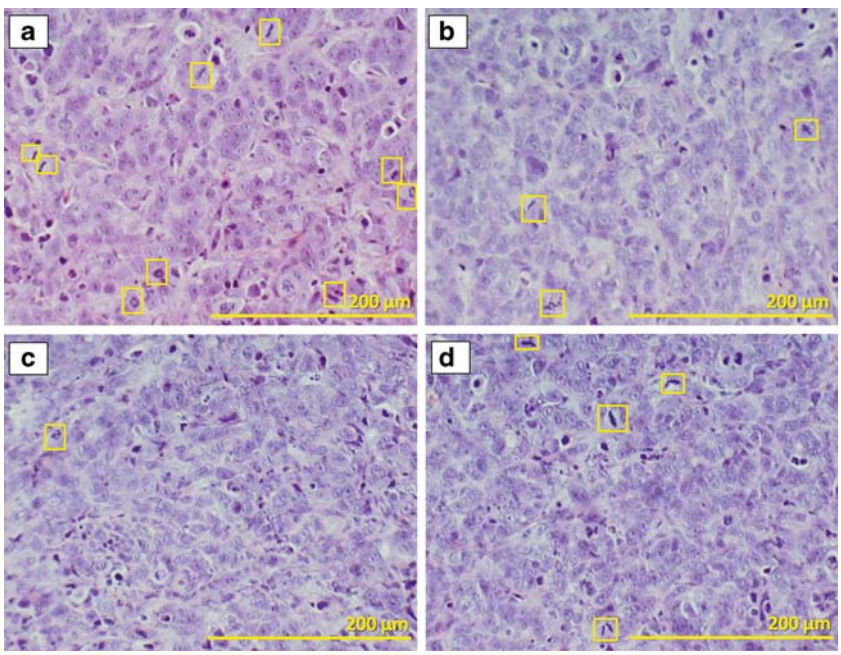

Fig. 3 Histological appearance of the epithelial-like cortex of MCF-7 cell untreated tumour (**a**), TMX-B-50-50 NP treated tumour (**b**), TMX-B-50-50-FOL NP treated tumour (**c**) and free TMX treated tumour (**d**), using the hematoxylin-eosin staining method (magnification 40X). Boxes indicate the presence of cells in different stages of mitotic division. *Yellow* bars represent 200 μm.

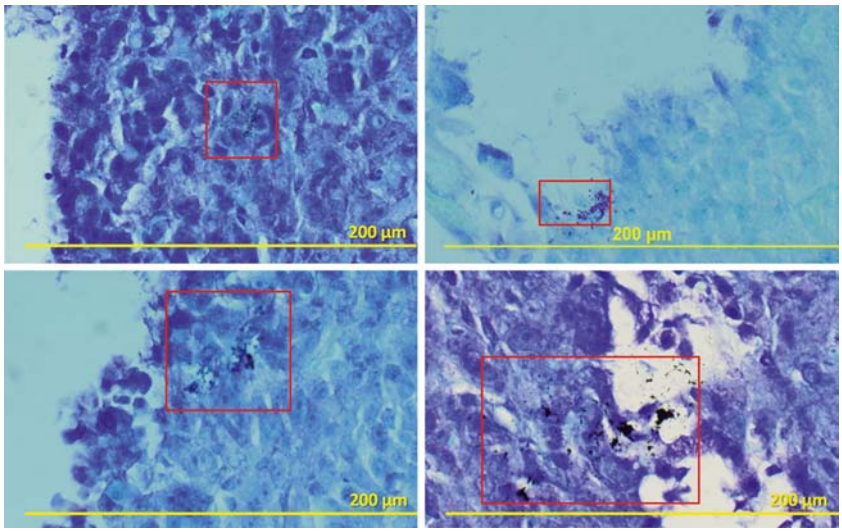

Fig. 4 Toluidine blue stained samples from TMX-B-50-50-FOL NP treated tumours where the presence of some residual TMX-B-50-50-FOL NP was evidenced. *Yellow* bars represent 200 μm.

the TMX biodistribution when it was administered in solution, or when it was given loaded in the NP.

Table III shows the concentration of TMX and 4OH-TMX in plasma and mice tissues after 12 days of treatment with free TMX and TMX-loaded nanoparticles. 4OH-TMX was detected in all liver and lung samples irrespective of the treatment, and significant differences were not found between them. It was also detected in the uterus and ovaries from free TMX treated mice, but was not detectable in the case of the uterus and ovaries coming from mice treated with TMX-loaded NP.

In the case of TMX biodistribution, detectable drug concentrations were obtained in all analysed tissues, with the exception of plasma samples. There was a high accumulation of TMX in the lungs, irrespective of the treatment. However, this value was significantly higher ($p < 0.05$) in the lung extract coming from free TMX treated mice than that from TMX-loaded NP treated groups (Table III). This situation was

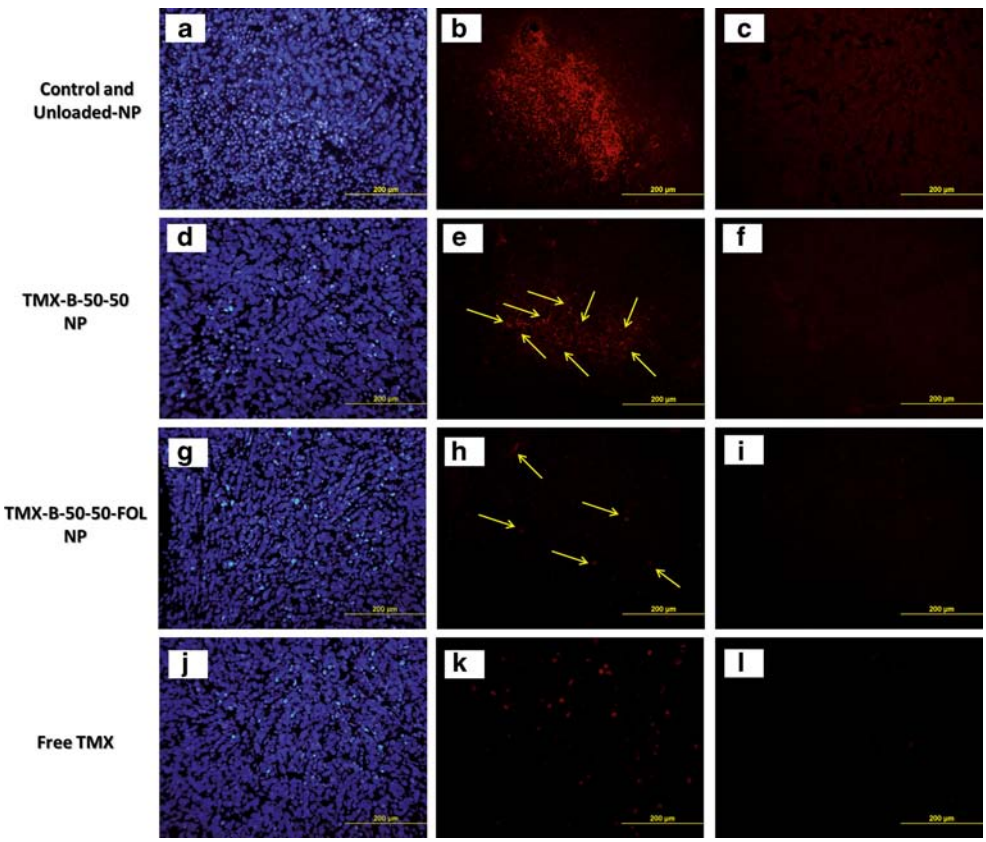

Fig. 5 Representative images of the immunohistochemical detection of Ki-67 antigen in MCF-7 xenograft tumour samples using a fluorescent method: control and placebo NP (**a** and **b**), TMX-B-50-50 NP (**d** and **e**), TMX-B-50-50-FOL NP (**g** and **h**) and free TMX (**j** and **k**) treated tumours; negative controls (**c**, **f**, **i** and **l**). In blue is represented the nuclear staining with DAPI. In red, the nuclear fluorescent signal due to the presence of Ki-67 proliferating antigen. Arrows indicate the presence of some Ki-67 positive nuclei in tumour tissue treated with TMX-loaded NP. *Yellow* bars represent 200 μm.

Table III Tamoxifen and 4-hydroxytamoxifen Concentrations in Serum and Tissues of Nude Mice After 12 days of Treatment with 4 μg TMX Administered Free and Trapped into Nanoparticles Every 3 Days

Group of treatment and tissues	TMX (ng TMX/g tissue)	4OH-TMX (ng TMX/g tissue)
Free TMX		
Plasma	–	–
Liver	21 ± 4**	70 ± 16
Lung	102 ± 10*	52 ± 2
Uterus and ovaries	23 ± 3**	16 ± 9**
Spleen	44 ± 4**	–
Kidneys	28 ± 5**	–
Tumour	11 ± 1	–
TMX-B-50-50-FOL NP		
Plasma	–	–
Liver	11 ± 1	49 ± 2
Lung	78.8 ± 0.3	47 ± 4
Uterus and ovaries	3.93 ± 0.6	–
Spleen	15.5 ± 0.6	–
Kidneys	7 ± 3	–
Tumour	8.6 ± 0.9	–
TMX-B-50-50 NP		
Plasma	–	–
Liver	10 ± 3	34 ± 11
Lung	82.6 ± 0.7	38 ± 4
Uterus and ovaries	3.4 ± 0.3	–
Spleen	12 ± 4	–
Kidneys	10 ± 4	–
Tumour	4.0 ± 0.6**	–

Data marked with * and ** showed significant ($p < 0.05$) and very significant ($p < 0.05$) statistical differences, respectively

repeated in the case of the liver, uterus and ovaries, spleen and kidneys, where TMX levels were very significantly higher ($p < 0.01$) than in organs from TMX-loaded NP treated group (Table III). TMX was similarly accumulated in the case of tumour tissues coming from free TMX and TMX-B-50-50-FOL NP treated mice, whereas very significantly lower values ($p < 0.01$) were obtained in the case of tumour tissues coming from the mice group treated with TMX-B-50-50 NP. Thus, the TMX accumulation in not-targeted tissues was significantly higher when the drug was administered freely than when it was trapped in NP. Additionally, TMX-B-50-50-FOL NP treatment achieved very similar TMX level in tumour samples to that achieved when TMX was administered as a solution.

DISCUSSION

Folic acid belongs to the family of vitamin B and is necessary to perform various metabolic reactions, including the biosynthesis of nucleotide bases. This vitamin is highly consumed by proliferating cells, such as those from several types of cancer cells, where folate receptor (FR) is over-expressed. FR has been used as a potential target for directed cancer treatments. It can also be considered as a target of intravenous anticancer drugs since it became accessible to targeted drugs in circulation after the malignant transformation of the cells, which causes changes in cell polarity (5). Folic acid is also especially interesting, in that it displays high binding affinity ($K_d \sim 10^{-10}$ M), low immunogenicity, ease of modification, small size, stability, compatibility with a variety of organic and aqueous solvents, low cost, and ready availability (16). It was for these reasons why folic acid molecule was selected to target tumour cells with TMX loaded into BSA-SH/ALG-CYS nanoparticles. TMX-B-50-50-FOL nanoparticles were characterized *in vitro* in a previous work (10), where they showed good results as controlled TMX delivery systems against different carcinoma cells. As the conclusion to this study showed, the combined effect of the attachment of folic acid to a NP structure and the presence of alginate in the NP composition was fundamental in enhancing the interaction between B-50-50-FOL NP and tumour cells. Consequently, an *in vivo* evaluation was considered necessary to test the use of this combination as a possible alternative to current TMX administration, and to compare its *in vivo* anticancer activity with free administered TMX and non-targeted nanoparticles.

The human oral dose of TMX (20 mg/day) (17) together with the absolute bioavailability value (AB%) of TMX calculated in rodents after oral administration (15 ± 4%) (18) were taken into account for determining the dose of TMX for this study. Considering the maximum value of AB% (19%) and an average mouse weight of 23 g, it was decided to administer a dose of 4 μg TMX every 3 days (1.3 μg TMX/day), which corresponded to 1 mg TMX-loaded NP every 3 days (0.3 mg NP/day).

The MCF-7 xenograft tumour in nude mice has been used as a common model for testing the *in vivo* anticancer activity of TMX (19,20), and some TMX derivatives (21). These studies revealed that the antiestrogen treatment with TMX normally resulted in cessation of tumour growth and subsequent tumour regression due to the cytostatic action of TMX. During the current study, tumour evolution was slowed down in the case of mice treated with TMX in solution and TMX-B-50-50-NP, whereas tumour regression was achieved with TMX-B-50-50-FOL-NP from the beginning of the treatment. Haran and co-workers (22) detected significant inhibition of tumour growth and significant tumour regression mostly after 2 weeks of treatment with TMX. In this way, treatment with TMX-B-50-50-FOL-NP allowed the tumour regression stage to be achieved earlier than with other TMX treatments. Although subcutaneous administration of TMX-B-50-50-NP was capable of enhancing the antitumor efficacy of TMX (9), the same formulation administered intravenously was not as

effective as the folate-targeted formulation. Consequently, active targeting of TMX together with the protection of the drug from degradation and passive targeting were successfully achieved when the drug was administered as TMX-B-50-50-FOL-NP. Similar results were obtained when other anticancer drugs were administered entrapped in folate-attached polymeric nanoparticles, resulting in enhancement of the efficacy of the treatment (23,24). Furthermore, unloaded NP seemed to stimulate tumour growth, especially in the case of B-50-50-FOL NP where the tumour growth rate doubled after treatment started. Previous cytocompatibility studies (7,10) performed with placebo B-50-50 NP and B-50-50-FOL NP against MCF-7 cultures revealed good cell viability results, and viability percentages were over 100% in some cases, even reaching values up to 110%. This might indicate that the polymeric composition itself could stimulate cell growth and would be responsible for the contribution to tumour growth development during the treatment with placebo NP. Consequently, TMX-B-50-50-FOL NP were able to counteract the proliferating effect of their own composition, and cause tumour regression, thus reinforcing the idea of their potential anticancer activity.

Histological analysis, using both routine and immunohistochemical staining methods, is a common procedure for obtaining useful pathological information, such as the structure and cell division stage of xenograft tumour tissues, (25,26). Tumour sections from mice treated with TMX-B-50-50-FOL-NP showed the most disorganized and quiescent tissues, with a low density of mitotic cells, which have been described as signs of tumour remission (27,28). Additionally, these tissues revealed the lowest presence of Ki-67 antigen, which has been considered to be a good prognostic sign, especially in breast cancer (29,30) These results, together with the capability of the systems to reach tumour sites after their systemic administration, suggested that TMX-B-50-50-FOL-NP was the most effective treatment. Wohlfart and co-workers (31) demonstrated the promising therapeutic potential of doxorubicin-loaded nanoparticles for systemic chemotherapy of human glioblastoma, and their results from histochemical and immunohistochemical studies were very similar to those obtained in the present study. The same conclusions were obtained from a study by Arias and co-workers (32) where gemcitabine was incorporated into chitosan nanoparticles, and where a more efficient drug action was observed.

Finally, the concentration of TMX and its metabolite, 4-OH-TMX, was measured in tumour, plasma, and other tissue samples in order to analyse the possible differences between the administration of free TMX or TMX-loaded nanoparticles. The absence of any of these molecules in plasma samples is in accordance with other previous studies where higher oral or subcutaneous doses of TMX were administered, and whereundetectable serum levels of TMX were also obtained (15,20). 4-OH-TMX was detected in the liver and the lungs of all mice. Although intravenous administration of TMX circumvents the first-pass metabolism in the liver, which is characteristic of the oral route, it was logical to expect high levels of 4-OH-TMX in this tissue since CYP3A family enzymes are mainly located in the liver and are responsible for TMX metabolism (33). The lungs were a large reservory of the drug and its metabolite. This fact was also observed in other TMX biodistribution studies (15,34), and it was justified by the high affinity of this tissue to the amine compunds (35). In uterine and ovarian samples TMX levels were 6 fold higher ($p < 0.01$) after free TMX treatment than after treatment by TMX entrapped in both types of nanoparticle. One of the most important undesirable effects resulting from TMX treatment is the possibility of developing an endometrial carcinoma, since TMX acts as an oestrogen-agonist in the uterus (36). So in this way, high uterine levels of TMX or 4-OH-TMX, which is even more active than TMX, could contribute to the development of endometrial cancer. The administration of TMX trapped in NP resulted in lower TMX and undetectable 4-OH-TMX uterine levels and, consequently, the probability of the development of the undesirable effect was reduced. Similar results were obtained in previous studies following the subcutaneous administration of TMX-loaded non-targeted nanoparticles (9). This means that the subcutaneous or intravenous administration of TMX, as either targeted or non-targeted BSA-SH/ALG-CYS NP, caused less accumulation in non-targeted organs, and especially in the uterus and ovaries, than when the drug was free administered. When TMX levels were analysed in the tumour samples, similar concentrations were obtained in the case of free TMX treated and TMX-B-50-50-FOL NP treated mice. These concentrations were very significantly higher ($p < 0.01$) than in the case of TMX-B-50-50 NP treated tumours. Despite the absence of statistical differences for TMX accumulation in tumour tissues between TMX-B-50-50-FOL NP and TMX in solution,, histological and immunohistochemical studies revealed that TMX-B-50-50-FOL NP treatment was much more effective than that of free TMX, unlike the case of free TMX this treatment was even able to cause tumour regression. Consequently, the same TMX concentration reached in tumour tissues showed an enhanced anticancer effect when it was administered using the targeted-nanoparticulated systems, and was less likely to produce undesirable side effects.

In conclusion, targeting TMX to tumour tissue through folate attachment to nanoparticles was scuccessfully achieved and appeared to be responsible for the tumour remission potential of the TMX-B-50-50-FOL formulation, and this confirms the potential of folic acid as a tumour-specific target as widely described in the literature. This work shows the important role of folic acid and its receptor in breast anticancer therapy, and raises the possibility of administering TMX trapped in folate-targeted polymeric nanosystems

through new administration routes, e.g. intravenously, with enhanced anticancer activity and less probability of undesirable side effect development.

ACKNOWLEDGMENTS AND DISCLOSURES

The authors are grateful to Dr. von Kobbe (Chimera Pharma of Bionostra Group) for the gift of MCF7 cells. The financial support of the Ministerio de Ciencia e Innovación of Spain (FIS PS09/01513 and MAT2010-21509-C03-03), and the FPI grant from UCM to A. Martínez are also gratefully acknowledged.

REFERENCES

1. Mahon E, Salvati A, Baldelli Bombelli F, Lynch I, Dawson KA. Designing the nanoparticle-biomolecule interface for "targeting and therapeutic delivery". J Control Release. 2012;161(2):164–74.
2. Wang M, Thanou M. Targeting nanoparticles to cancer. Pharmacol Res. 2010;62(2):90–9.
3. Cazzaniga M, Bonanni B. Breast cancer chemoprevention: old and new approaches. J Biomed Biotechnol. 2012;2012:985620.
4. Brigger I, Dubernet C, Couvreur P. Nanoparticles in cancer therapy and diagnosis. Adv Drug Deliv Rev. 2002;54(5):631–51.
5. Lu Y, Low PS. Folate-mediated delivery of macromolecular anticancer therapeutic agents. Adv Drug Deliv Rev. 2002;54(5):675–93.
6. Gao W, Xiang B, Meng TT, Liu F, Qi XR. Chemotherapeutic drug delivery to cancer cells using a combination of folate targeting and tumor microenvironment-sensitive polypeptides. Biomaterials. 2013;34(16):4137–49.
7. Martinez A, Benito-Miguel M, Iglesias I, Teijon JM, Blanco MD. Tamoxifen-loaded thiolated alginate-albumin nanoparticles as antitumoral drug delivery systems. J Biomed Mater Res A. 2012;100A(6):1467–76.
8. Martínez A, Iglesias I, Lozano R, Teijón JM, Blanco MD. Synthesis and characterization of thiolated alginate-albumin nanoparticles stabilized by disulfide bonds. Evaluation as drug delivery systems. Carbohydr Polym. 2011;83(3):1311–21.
9. Martinez A, Muniz E, Iglesias I, Teijon JM, Blanco MD. Enhanced preclinical efficacy of tamoxifen developed as alginate-cysteine/disulfide bond reduced albumin nanoparticles. Int J Pharm. 2012;436(1–2):574–81.
10. Martínez A, Olmo R, Iglesias I, Teijon JM, Blanco MD. Folate-targeted nanoparticles based on albumin/alginate mixtures as controlled release systems of tamoxifen. Synthesis and iIn vitro characterization Pharmaceutical Research. 2013; Accepted *(In Press)*.
11. Lee RJ, Low PS. Delivery of liposomes into cultured KB cells via folate receptor-mediated endocytosis. J Biol Chem. 1994;269(5):3198–204.
12. Behrens D, Gill JH, Fichtner I. Loss of tumourigenicity of stably ERbeta-transfected MCF-7 breast cancer cells. Mol Cell Endocrinol. 2007;274(1–2):19–29.
13. Humason GL, editor. Animal Tissue Techniques. 4th ed. New York 1979.
14. Patel VR, Amiji MM. Preparation and characterization of freeze-dried chitosan-poly(ethylene oxide) hydrogels for site-specific antibiotic delivery in the stomach. Pharm Res. 1996;13(4):588–93.
15. Kisanga ER, Gjerde J, Schjott J, Mellgren G, Lien EA. Tamoxifen administration and metabolism in nude mice and nude rats. J Steroid Biochem Mol Biol. 2003;84(2–3):361–7.
16. Reddy JA, Low PS. Folate-mediated targeting of therapeutic and imaging agents to cancers. Crit Rev Ther Drug Carrier Syst. 1998;15(6):587–627.
17. Lee KH, Ward BA, Desta Z, Flockhart DA, Jones DR. Quantification of tamoxifen and three metabolites in plasma by high-performance liquid chromatography with fluorescence detection: application to a clinical trial. J Chromatogr B Analyt Technol Biomed Life Sci. 2003;791(1–2):245–53.
18. Shin SC, Choi JS, Li X. Enhanced bioavailability of tamoxifen after oral administration of tamoxifen with quercetin in rats. Int J Pharm. 2006;313(1–2):144–9.
19. Long BJ, Jelovac D, Handratta V, Thiantanawat A, MacPherson N, Ragaz J, *et al*. Therapeutic strategies using the aromatase inhibitor letrozole and tamoxifen in a breast cancer model. J Natl Cancer Inst. 2004;96(6):456–65.
20. Osborne CK, Hobbs K, Clark GM. Effect of estrogens and antiestrogens on growth of human breast cancer cells in athymic nude mice. Cancer Res. 1985;45(2):584–90.
21. Laine AL, Adriaenssens E, Vessieres A, Jaouen G, Corbet C, Desruelles E, *et al*. The in vivo performance of ferrocenyl tamoxifen lipid nanocapsules in xenografted triple negative breast cancer. Biomaterials. 2013;34(28):6949–56.
22. Haran EF, Maretzek AF, Goldberg I, Horowitz A, Degani H. Tamoxifen enhances cell death in implanted MCF7 breast cancer by inhibiting endothelium growth. Cancer Res. 1994;54(21):5511–4.
23. Zhao P, Wang H, Yu M, Liao Z, Wang X, Zhang F, *et al*. Paclitaxel loaded folic acid targeted nanoparticles of mixed lipid-shell and polymer-core: in vitro and in vivo evaluation. Eur J Pharm Biopharm. 2012;81(2):248–56.
24. Hao HQ, Ma QM, Huang C, He F, Yao P. Preparation, characterization, and in vivo evaluation of doxorubicin loaded BSA nanoparticles with folic acid modified dextran surface. Int J Pharmaceut. 2013;444(1–2):77–84.
25. Fernandez SV, Robertson FM, Pei J, Aburto-Chumpitaz L, Mu Z, Chu K, *et al*. Inflammatory breast cancer (IBC): clues for targeted therapies. Breast Cancer Res Treat. 2013 Jun 21.
26. Stuelten CH, Busch JI, Tang B, Flanders KC, Oshima A, Sutton E, *et al*. Transient tumor-fibroblast interactions increase tumor cell malignancy by a TGF-Beta mediated mechanism in a mouse xenograft model of breast cancer. PLoS One. 2010;5(3):e9832.
27. Bani D, Flagiello D, Poupon MF, Nistri S, Poirson-Bichat F, Bigazzi M, *et al*. Relaxin promotes differentiation of human breast cancer cells MCF-7 transplanted into nude mice. Virchows Arch. 1999;435(5):509–19.
28. Lee HJ, Seo NJ, Jeong SJ, Park Y, Jung DB, Koh W, *et al*. Oral administration of penta-O-galloyl-beta-D-glucose suppresses triple-negative breast cancer xenograft growth and metastasis in strong association with JAK1-STAT3 inhibition. Carcinogenesis. 2011;32(6):804–11.
29. Shahzad MM, Mangala LS, Han HD, Lu C, Bottsford-Miller J, Nishimura M, *et al*. Targeted delivery of small interfering RNA using reconstituted high-density lipoprotein nanoparticles. Neoplasia. 2011;13(4):309–19.
30. Pathmanathan N, Balleine RL. Ki67 and proliferation in breast cancer. J Clin Pathol. 2013;66(6):512–6.
31. Wohlfart S, Bernreuther C, Khalansky AS, Theisen A, Weissenberger J, Gelperina S, *et al*. Increased numbers of injections of doxorubicin bound to nanoparticles lead to enhanced efficacy against rat glioblastoma 101/8. J Nanoneurosci. 2009;1(2):144–51.
32. Arias JL, Reddy LH, Couvreur P. Superior preclinical efficacy of gemcitabine developed as chitosan nanoparticulate system. Biomacromolecules. 2011;12(1):97–104.

33. Cotreau MM, von Moltke LL, Harmatz JS, Greenblatt DJ. Molecular and pharmacokinetic evaluation of rat hepatic and gastrointestinal cytochrome p450 induction by tamoxifen. Pharmacology. 2001;63(4):210–9.
34. Wilking N, Appelgren LE, Carlstrom K, Pousette A, Theve NO. The distribution and metabolism of 14C-labelled tamoxifen in spayed female mice. Acta Pharmacol Toxicol (Copenh). 1982;50(3):161–8.
35. Bend JR, Serabjit-Singh CJ, Philpot RM. The pulmonary uptake, accumulation, and metabolism of xenobiotics. Annu Rev Pharmacol Toxicol. 1985;25:97–125.
36. Gao WL, Zhang LP, Feng LM. Comparative study of transvaginal ultrasonographic and diagnostic hysteroscopic findings in postmenopausal breast cancer patients treated with tamoxifen. Chin Med J (Engl). 2011;124(15):2335–9.